4-28-2014

Reconstruction of Pacific Ocean Bottom Water Salinity During the Last Glacial Maximum

Tania Lado Insua

Arthur J. Spivack
University of Rhode Island, spivack@uri.edu

Dennis Graham

Steven D'Hondt
University of Rhode Island, dhondt@uri.edu

Kathryn Moran

Citation/Publisher Attribution

Insua, T.L.; Spivack, A.J.; Graham, D.; D'Hondt, S.; Moran, K. (2014). "Reconstruction of Pacific Ocean bottom water salinity during the Last Glacial Maximum." Geophysical Research Letters. 41(8): 2914-20. Available at: http://dx.doi.org/10.1002/2014GL059575

Reconstruction of Pacific Ocean Bottom Water Salinity During the Last Glacial Maximum

AGU PUBLICATIONS

Geophysical Research Letters

RESEARCH LETTER
10.1002/2014GL059575

Key Points:
- LGM salinity of Pacific bottom water was 4.09 ± 0.4% greater than today
- The salinity of bottom waters was homogeneous across latitudes studied
- Based on sea level, salinity reconstructions were higher than expected values

Supporting Information:
- Readme
- Figure S1
- Text S1

Correspondence to:
T. L. Insua,
tinsua@uvic.ca

Citation:
Insua, T. L., A. J. Spivack, D. Graham, S. D'Hondt, and K. Moran (2014), Reconstruction of Pacific Ocean bottom water salinity during the Last Glacial Maximum, *Geophys. Res. Lett.*, *41*, 2914–2920, doi:10.1002/2014GL059575.

Received 10 FEB 2014
Accepted 26 MAR 2014
Accepted article online 29 MAR 2014
Published online 28 APR 2014

Reconstruction of Pacific Ocean bottom water salinity during the Last Glacial Maximum

Tania Lado Insua[1], Arthur J. Spivack[2], Dennis Graham[2], Steven D'Hondt[2], and Kathryn Moran[1,2]

[1]Ocean Networks Canada, University of Victoria, Victoria, British Columbia, Canada, [2]Graduate School of Oceanography, University of Rhode Island, Narragansett, Rhode Island, USA

Abstract Knowledge of salinity in the deep ocean is important for understanding past ocean circulation and climate. Based on sedimentary pore fluid chloride measurements of a single Pacific site, Adkins et al. (2002) suggested that, during the Last Glacial Maximum (LGM), the Pacific deep bottom water was saltier than expected based on lower sea level alone. Here we present high-resolution salinity profiles from five sites in the South, Equatorial, and North Pacific Ocean. Our study greatly constrains understanding of LGM salinity in the Pacific Ocean. Our results show that LGM chloride concentrations of deep Pacific bottom water were 4.09 ± 0.4% greater than today's values. Pacific Ocean bottom water salinity was also indistinguishable from being homogeneous across the wide range of latitudes studied here. These LGM salinity reconstructions are on average slightly higher (~1.4 to 1% higher) than expected from sea level of the time, which is generally inferred to have been ~120 to ~135 m lower than today.

1. Introduction

The meridional overturning circulation (MOC) directly impacts climate via its heat transport [e.g., *Srokosz et al.*, 2012] and the sequestration of CO_2 [e.g., *Ito and Follows*, 2005; *Intergovernmental Panel on Climate Change*, 2007; *Zickfeld et al.*, 2012; *Skinner et al.*, 2010]. For these reasons, identifying its variation and understanding its driving mechanisms are areas of active research. There are various hypotheses about the MOC's future and past patterns [*McManus et al.*, 2004; *Meissner*, 2007; *Okazaki et al.*, 2010; *Lippold et al.*, 2012; *Ritz et al.*, 2013]. Although it is generally accepted that deep-ocean circulation can attain different equilibrium states, uncertainty remains about which will emerge in response to climate change [Stommel, 1961; reviewed in *Kuhlbrodt et al.*, 2007]. Variations in the MOC are strongly affected by changes in density generated by temperature and salinity variations [e.g., *Bryden et al.*, 2005].

Reconstruction of past deep-ocean conditions enables a better understanding of how ocean circulation has changed and could change in the future in response to climate change. Deep-ocean circulation is often studied by direct measurements of salinity and temperature because they affect density and therefore geostrophic flow. Salinity and temperature are also used to identify water masses and circulation patterns [*Wüst*, 1935; *Sverdrup et al.*, 1961]. *McDuff* [1984, 1985] pointed out that the salinity of the Last Glacial Maximum (LGM) is preserved in marine sediment pore fluid. *Schrag and DePaolo* [1993] and, later, *Adkins and Schrag* [2001] successfully built on this idea and reconstructed both salinity and temperature (via oxygen isotopes) of the LGM ocean at a limited number of locations. Based on these results [*Schrag et al.*, 1996, 2002; *Adkins and Schrag*, 2001, 2003; *Adkins et al.*, 2002], they argue that (i) the glacial-age deep ocean's density structure was dominated by salinity variations, rather than temperature variations, as it is today, and (ii) the ocean was more strongly salinity stratified.

Presently, Pacific bottom waters are renewed by the flow of Lower Circumpolar Deep Water (LCDW) from the Antarctic Circumpolar Current System (ACCS) [e.g., *Talley et al.*, 2011]. This water enters the Pacific as a deep western boundary current, in the southwestern part of the basin, east of New Zealand. The LCDW is the major water source for the entire basin and there is only a small salinity decrease from the bottom waters of the South Pacific to the North Pacific, due to diapycnal mixing of fresher overlying water. Repeated circulation in the ACCS, where the North Atlantic Deep Water and the Antarctic Bottom Water mix to become LCDW, homogenizes this water mass [*Schmitz*, 1996]. The nearly uniform composition of today's Pacific bottom water is due to the uniformity of this source. No bottom waters presently form in the Pacific; however, it is unclear that the locations where water masses formed during the LGM were the same as today [*Ganopolski*

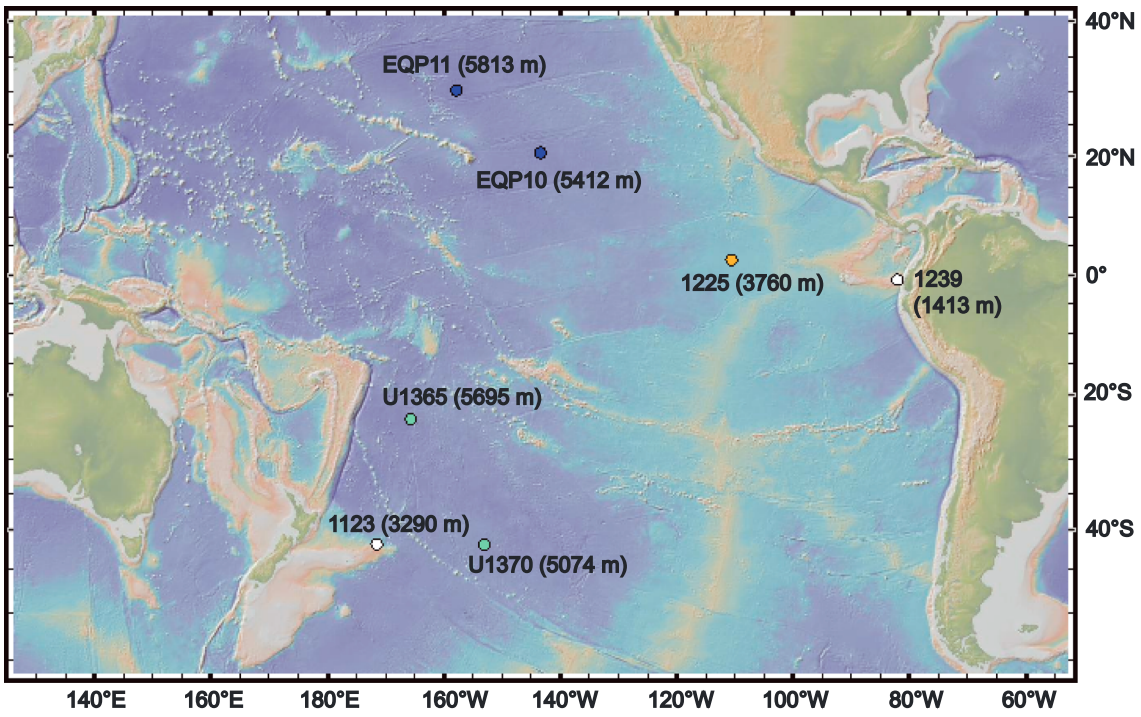

Figure 1. Bathymetric map of the sites used for this study. Water depth of the site is indicated in parenthesis. Blue indicates sites from expedition KN-195 (III), orange indicates ODP Leg 201 sites, and green indicates IODP Expedition 329 sites. For comparison, white indicates Sites 1123 (ODP Leg 202) and 1239 (ODP Leg 181) previously reported by *Adkins et al.* [2002] and *Adkins and Schrag* [2003].

and Rhamstorf, 2001; *Lynch-Stieglitz et al.*, 2007; *Toggweiler and Russell*, 2008; *Okazaki et al.*, 2010; *Skinner et al.*, 2010; *Kwon et al.*, 2012].

Although a saltier and more stratified deep glacial ocean has been reported [*Lea et al.*, 2000; *Adkins and Schrag*, 2001, 2003; *Adkins and Pasquero*, 2004; *Lynch-Stieglitz et al.*, 2007; *Herguera et al.*, 2010], reconstruction of ocean salinity during the LGM, globally, has not yet been realized. The results to date are important [*Adkins and Schrag*, 2001, 2003; *Schrag et al.*, 1996, 2002] but include only two Pacific sites: Ocean Drilling Program (ODP) Site 1123 [*Adkins et al.*, 2002] and ODP Site 1239 [*Adkins and Schrag*, 2003] (Figure 1). Site 1123 is located on the margin of the Southern Ocean [*Shipboard Scientific Party*, 1999] and Site 1239 in the eastern boundary of the Pacific [*Shipboard Scientific Party*, 2003]. Site 1123, 3290 m water depth, is located in the region where a deep western boundary current presently supplies the bottom water of the Pacific with LCDW. Site 1239 is relatively shallow, 1423 m, and therefore is not representative of deep Pacific bottom water.

If the data from Site 1123 are reliable and LGM bottom waters of the Pacific circulated similarly to today, LGM bottom waters throughout the Pacific should have been similar in salinity to Site 1123. The uncertainty indicated by *Adkins et al.* [2002] for reconstructed salinity at this site addresses the model error mainly due to the scatter in the measured data. We expand on their study by using sediment pore fluid measurements, coupled with diffusion modeling, to reconstruct salinity during the LGM in five locations that span the bottom waters of the Equatorial Pacific, the South Pacific gyre, and the North Pacific gyre (Figure 1). Our calculations also include a statistical analysis based on a Student's *t* distribution of the chlorinity model results for all sites that allows us to estimate the 90% confidence interval of the result to determine the uncertainty of this methodology.

2. Materials and Methods: Reconstructing Paleosalinities

We collected sedimentary pore water samples from five sites during three separate cruises: R/V *Knorr* 195 (III) (Sites EQP10 and EQP11), ODP Leg 201 (Site 1225), and IODP Expedition 329 (Sites U1365 and U1370). Sites

EQP10 and EQP11 were collected with long piston cores, while the other sites were drilled and cored. These samples cover deep areas (>3760 m water depth) of the Pacific basin in the eastern Equatorial Pacific, the North Pacific gyre, and the South Pacific gyre (Figure 1). Core recovery was high in all cases (>90%). The recovered sediment was dominated by abyssal clay (EQP10, EQP11, U1365, and U1370) and carbonate ooze (1225). Two of the sites were drilled to the basaltic basement (1225 and U1370), and one (U1365) contained an impermeable chert layer. At the two remaining sites (EQP10 and EQP11), the numerical model for reconstructing salinity was extrapolated to 100 m below seafloor (mbsf), the estimated approximate depth to basalt based on seismic reflection profiles. At sites EQP10 and EQP11, our chloride concentration measurements only reach a depth of ~27 mbsf, yet the column of sediment (~100 m) was thick enough to model chloride concentration for the LGM. Despite reaching only 27 mbsf, the modeled salinity results quantitatively constrain LGM salinity. An in-depth description, justifying the use of these sites and of the assumptions in our model, is presented in the supporting information.

Sediment interstitial water was collected by squeezing whole core rounds [*Manheim and Sayles*, 1974], and chloride concentration was determined. Porosity and formation factor were also determined through the entire cores. Details of the sampling and analytical methods are given in the supporting information. Measured chloride concentrations are shown as equivalent salinities in all graphs. At all sites, salinity describes a curve with a peak that corresponds to the signal from the LGM as the low-salinity interglacial water diffuses down through the sediment. The maximum is expected at approximately 40 mbsf for all of our study sites, based on the diffusion model presented here, which takes into account the measured porosity and tortuosity values of these sites (see supporting information for more detail). We conducted numerical sensitivity tests to detect the depth at which 90% of the maximum is reached. Sites that have a sediment thickness of ~50 m or greater and a core recovery of ~25 m or greater will reach at least 90% of the maximum [*Adkins et al.*, 2002].

The linear diffusion rate depends on sediment porosity and tortuosity [*Boudreau*, 1996a, 1996b]. In previous paleosalinity studies, tortuosity was estimated from measured porosity using variants of Archie's law [e.g., *Adkins and Schrag*, 2003]. In contrast, we use measured formation factors to infer tortuosity for all sites, except Site 1225, where tortuosity was not measured; for this site we used Archie's law [*Archie*, 1947]. Changes in diffusivity due to temperature were taken into account following the Stokes-Einstein relation.

Similar to previous studies, we use a one-dimensional, time-dependent, numerical diffusion model to find the magnitude of LGM salinity that best fits the measured data

$$\phi \frac{\partial C}{\partial t} = \frac{\partial}{\partial z}\left(\frac{\phi D}{\theta^2}\frac{\partial C}{\partial z}\right) = \frac{\partial}{\partial z}\left(\frac{D}{f}\frac{\partial C}{\partial z}\right)$$

where C is the chloride concentration, t is time, z is depth below the sediment-water interface, ϕ is porosity, θ^2 is tortuosity, D is the free solution chloride diffusion coefficient, 1.00×10^{-9} (m^2/s) at 2.5°C [*Boudreau*, 1996a, 1996b], and f is formation factor. We implemented the diffusion equation in MATLAB. All sites are dominated by low sedimentation rates (~0.3 mm/ka), and therefore, their Peclet numbers are too small ($<1.6 \times 10^{-3}$) to produce significant advection compared to diffusion. We added no reaction term to the equation, because our sites are dominated by abyssal clay and biogenic ooze far from volcanic areas and therefore free of buried unreactive ash that could react and alter the chloride values [*Adkins and Schrag*, 2003]. The chert layer at U1365 does not appear to affect the chloride values either as evidenced by the lack of a concentration gradient at its top interface. Details of the model and assumptions are provided in the supporting information.

The parameter that we optimize is the chloride concentration of the bottom water as a function of time; we refer to it as the bottom water boundary condition (BWBC). Its relative variation with time is based on reconstructed sea level variation, but its magnitude is optimized by a factor, α, to best fit to the measured pore water profile (see supporting information for a detailed description). We used the sea level curve described by *Adkins and Schrag* [2003] based on the coral sea level data for the last 30,000 years [*Fairbanks*, 1989; *Bard et al.*, 1990; *Edwards et al.*, 1993] and the deep water record of *Chappell and Shackleton* [1986] from 115 ky to the present. We optimized the BWBC by minimizing the mean square error between the modeled and measured data. The three most important parameters that affect the accuracy of this reconstruction are diffusivity (improved here with the use of measured formation factors), scatter in measured chloride concentration, and uncertainty in the input BWBC [*Adkins and Schrag*, 2003].

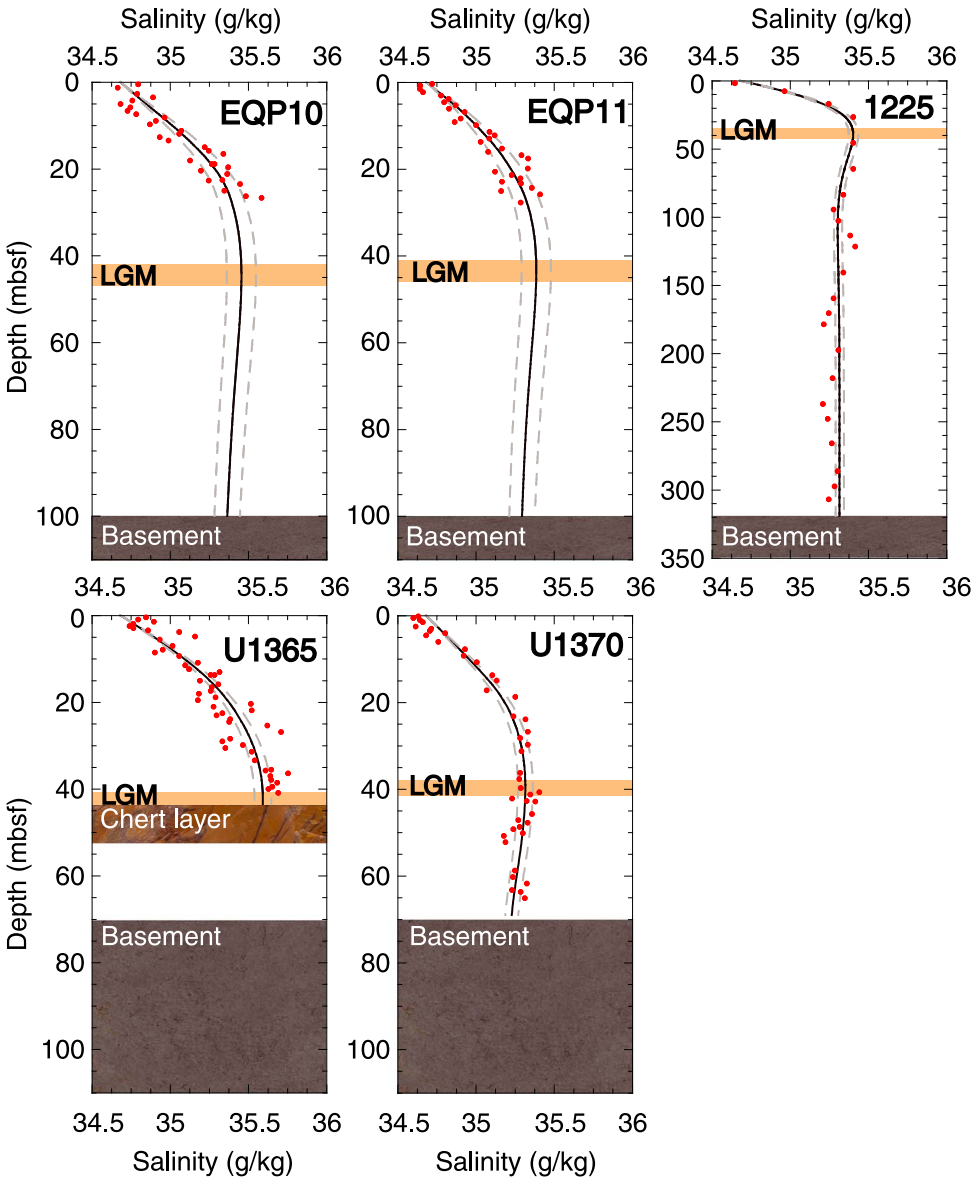

Figure 2. Salinity profiles plotted with depth below seafloor for our six sites. Optimized (α) modeled salinity curve (black line); salinity curve error (grey dashed lines) produced by $\alpha \pm 0.1$ for all sites, except EQP10 and EQP11 where $\alpha \pm 0.2$, and measured salinity based on chloride concentration (red dots).

The numerical analysis also requires initial conditions and an additional boundary condition: (1) an initial chloride concentration profile and (2) a boundary condition at the bottom of the profile. For consistency, we used an iterative method, where the initial condition of the model was the average of chloride concentration for the last 115 ky based on the optimized sea level curve and the α value; however, the model is relatively insensitive to the initial condition for the depths where the LGM signal is captured [*Adkins and Schrag*, 2003].

We used two different boundary conditions for the bottom of the sediment column: a concentration boundary condition at Sites 1225, EQP10, EQP11, and U1370 (equal to the initial condition of the model) and a no-flux bottom boundary condition for Site U1365 (where the chert layer occurs).

3. Results and Discussion

Our salinity profiles reconstructed from the one-dimensional diffusion model closely match the measured values throughout the depth profile at each site (Figure 2). This result differs from previous studies, which

Table 1. Site Information, Modern, and Reconstructed LGM Values for Chloride Concentration and Salinity and Relative Difference of LGM Salinity Compared to Modern Salinity

Site Information (North to South)				Modern Values		LGM Values		
Site	Latitude	Longitude	Water Depth (m)	Chloride Concentration (mM)	Salinity (g/kg)[a]	Chloride Concentration (mM)	Salinity (g/kg)	Relative Difference LGM Salinity Compared to Modern
EQP11	30.355	−157.871	5813	551.26	34.69	576.37 ± 2.93	36.06 ± 0.18	4.41 ± 0.5
EQP10	20.683	−143.357	5412	551.42	34.70	578.86 ± 2.93	36.21 ± 0.18	3.96 ± 0.5
ODP 1225	2.771	−110.571	3760	551.26	34.69	576.66 ± 1.46	36.07 ± 0.09	4.01 ± 0.3
IODP U1365	−23.851	−165.644	5695	551.42	34.70	579.52 ± 1.46	36.25 ± 0.09	4.53 ± 0.3
IODP U1370	−41.852	−153.106	5074	551.58	34.71	574.03 ± 1.46	35.91 ± 0.09	3.54 ± 0.3

[a]Salinity obtained from the WOCE atlas closest line.

identified the absence of tortuosity data as a potential cause of mismatch [*Adkins and Schrag*, 2003]. The reconstructed LGM bottom water salinities ranged from 35.91 to 36.25g/kg (Table 1) with a corrected standard deviation of 0.39 g/kg. This is equivalent to salinity values between ~3.54% and ~4.53% higher than today's Pacific bottom water (Table 1). Since the variation between sites is not geographically correlated, the range most likely reflects uncertainty due to the method. The salinity of the bottom water for these sites today range from 34.69 to 34.71 g/kg (World Ocean Circulation Experiment (WOCE) database, Table 1). Thus, at the 90% confidence level based on a Student's *t* distribution, using all our sites, the mean value of the reconstructed LGM Pacific bottom water salinity is 36.10 ± 0.10 g/kg or 4.09 ± 0.3% greater than present.

The standard deviation between sites places a limit on the total methodological uncertainty. If the sites are homogeneous, then the standard deviation is due to the uncertainty of the method. If there is a significant difference between sites, some of the variance can be attributed to this difference and the uncertainty due to the method would be smaller.

Site U1365 has an impermeable chert layer close to the depth where the LGM signal is expected to reach its maximum. Sedimentary marine chert composed of opal-A is known to contain up to 13% water [*Keene*, 1976]. If chert is still actively forming at this site, there is potential for an artifact in the chloride profile due to water loss to the chert and we would expect a chloride gradient at the chert interface. However, although no gradient is observed, we think the results at this site should be accepted with some caution. The mean value excluding this site is 36.06 ± 0.12 (90% confidence level) or 3.98 ± 0.3% greater than present.

The argument that the ocean had greater salinity stratification during the LGM rests on comparison of reconstructed LGM salinities to LGM salinities expected due solely to changes in sea level [*Adkins et al*., 2002]. Estimates of average global sea level for the LGM fall in a range [e.g., *Milne and Mitrovica*, 2008]. These vary from ~120 m lower than today [*Fairbanks*, 1989; *Bard et al*., 1990; *Lambeck et al*., 2002; *Peltier and Fairbanks*, 2006] to ~135 m lower or more, as reported by *Colonna et al*. [1996] and *Yokoyama et al*. [2000]. Based on a LGM sea level of −120 to −135 m current salinity values for Pacific bottom waters [*WOCE Database*, 2013], and the average depth for the modern ocean of 3682 m [*Charette and Smith*, 2010], the LGM salinity range expected, if the salinity only varied due to sea level changes, is 35.83 to 35.97 g/kg, 3.26 to 3.66% higher than today. These values are ~0.1% greater than previously used in a similar calculation [*Adkins et al*., 2002] due to the use of a more recent estimate of average ocean depth.

4. Conclusions

We have reconstructed the salinity of Pacific bottom water during the Last Glacial Maximum (LGM) with data and model results from five new sites spanning the South, Equatorial, and North Pacific. Our analysis of numerous sites allows us to constrain the uncertainty of the paleo–pore fluid technique to reconstruct past salinity. The mean value for all of our sites indicates consistent LGM salinity over a wide geographic region of the Pacific Ocean. Our mean value, 36.10 ± 0.10 g/kg (36.06 ± 0.12 if Site U1365 is excluded), is consistent with the value previously reported for ODP Site 1123, 36.19 ± 0.07 [*Adkins et al*., 2002], in the region where bottom water is presently supplied to the Pacific basin. Our mean value is 4.09 ± 0.4% greater than present-day salinity. This value is slightly higher than those predicted based solely on most estimates of sea level during

the LGM (3.26 to 3.66%) [*Adkins et al*., 2002]. However, if sea level was only slightly lower [*Colonna et al*., 1996], changes in sea level would suffice to explain our mean bottom water Pacific value for the LGM.

Thus, our results support the accuracy of the Site 1123 results and are consistent with the bottom waters of the Pacific being supplied by a homogenous water mass as it is today. This consistency implies that the primary mechanism that drives Pacific bottom water uniformity today, the ACCS, was active enough to homogenize Pacific bottom water salinity during the LGM.

Acknowledgments

The authors want to thank the Barrié de La Maza Foundation, IODP-MI, and NSF for its financial support to Tania Lado Insua during the development of this study. We would like to thank Christian Janssen and Jeffrey Harris for their useful code reviews. We thank the crew, science party, and technical staff of IODP Expedition 329 and *Knorr* 195 (III). This research uses samples and data provided by the Integrated Ocean Drilling Program. The IODP is sponsored by the U.S. National Science Foundation (NSF) and participating countries.

The Editor thanks an anonymous reviewer for assisting in the evaluation of this paper.

References

Adkins, J. F., and C. Pasquero (2004), Deep ocean overturning—Then and now, *Science*, *306*, 1143–1144.

Adkins, J. F., and D. P. Schrag (2001), Pore fluid constraints on deep ocean temperature and salinity during the last glacial maximum, *Geophys. Res. Lett.*, *28*(5), 771–774.

Adkins, J. F., and D. P. Schrag (2003), Reconstructing the Last Glacial Maximum bottom water salinities from deep-sea sediment pore fluid profiles, *Earth Planet. Sci. Lett.*, *216*, 109–123.

Adkins, J. F., K. McIntyre, and D. P. Schrag (2002), The salinity, temperature, and δ^{18}O of the Glacial Deep Ocean, *Science*, *298*, 1769–1773.

Archie, G. E. (1947), Electrical resistivity an aid in core analysis interpretation, *Am. Assoc. Pet. Geol. Bull.*, *31*(2), 350–366.

Bard, E., B. Hamelin, and R. G. Fairbanks (1990), U-Th ages obtained by mass spectrometry in corals from Barbados: Sea level during the past 130,000 years, *Nature*, *346*, 456–458.

Boudreau, B. P. (1996a), *Diagenetic Models and Their Implementation*, Springer, New York.

Boudreau, B. P. (1996b), The diffusive tortuosity of fine-grained unlithified sediments, *Geochim. Cosmochim. Acta*, *60*, 3139–3142.

Bryden, H. L., H. R. Longworth, and S. A. Cunningham (2005), Slowing of the Atlantic meridional overturning circulation at 25°N, *Nature*, *438*(1), 655–657.

Chappell, J., and N. J. Shackleton (1986), Oxygen isotopes and sea level, *Nature*, *324*, 137–140.

Charette, M. A., and W. H. Smith (2010), The volume of Earth's ocean, *Oceanography*, *23*(2), 112–114.

Colonna, M., J. Casanova, W.-C. Dullo, and G. Camoin (1996), Sea-level changes and δ^{18}O record for the past 34,000 yr from Mayotte Reef, Indian Ocean, *Quat. Res.*, *46*, 335–339.

Edwards, L. R., J. W. Beck, G. S. Burr, D. J. Donahue, J. M. A. Chappell, A. L. Bloom, E. R. M. Druffel, and F. W. Taylor (1993), A large drop in atmospheric $^{14}C/^{12}C$ and reduced melting in the Younger Dryas, documented with ^{230}Th ages of corals, *Science*, *260*(5110), 962–968.

Fairbanks, R. G. (1989), A 17,000-year glacio-eustatic sea level record: Influence of glacial melting rates on the Younger Dryas event and deep-ocean circulation, *Nature*, *342*, 637–642.

Ganopolski, A., and S. Rhamstorf (2001), Rapid changes of glacial climate simulated in a coupled climate model, *Nature*, *409*(11), 153–158.

Herguera, J. C., T. Herbert, M. Kashgarian, and C. Charles (2010), Intermediate and deep water mass distribution in the Pacific during the last glacial maximum inferred from oxygen and carbon stable isotopes, *Quat. Sci. Rev.*, *29*, 1228–1245.

Intergovernmental Panel on Climate Change (2007), *Climate Change 2007: The Physical Science Basis*, *Contribution of Working Group I to the Fourth Assessment Report of the Intergovernmental Panel on Climate Change*, edited by S. Solomon et al., Cambridge Univ. Press, Cambridge, U. K.

Ito, T., and M. J. Follows (2005), Preformed phosphate, soft tissue pump and atmospheric CO_2, *J. Mar. Res.*, *63*, 813–839.

Keene, J. B. (1976), The distribution, mineralogy, and petrology of biogenic and authigenic silica from the Pacific Basin, PhD dissertation, 264 pp., Scripps Institution of Oceanography, La Jolla, Calif.

Kuhlbrodt, T., A. Griesel, M. Montoya, A. Levermann, M. Hofmann, and S. Rahmstorf (2007), On the driving processes of the Atlantic meridional overturning circulation, *Rev. Geophys.*, *45*, RG2001, doi:10.1029/2004RG000166.

Kwon, E. Y., M. P. Hain, D. M. Sigman, E. D. Galbraith, J. L. Sarmiento, and J. R. Toggweiler (2012), North Atlantic ventilation of "southern-sourced" deep water in the glacial ocean, *Paleoceanography*, *27*, PA2208, doi:10.1029/2011PA002211.

Lambeck, K., Y. Yokoyama, and T. Purcell (2002), Into and out of the Last Glacial Maximum: Sea-level change during Oxygen Isotope Stages 3 and 2, *Quat. Sci. Rev.*, *21*(1), 343–360.

Lea, D. W., D. K. Pak, and H. J. Spero (2000), Climate impact of late Quaternary equatorial Pacific sea surface temperature variations, *Science*, *289*, 1719–1724.

Lippold, J., Y. Luo, R. Francois, S. E. Allen, J. Gherardi, S. Pichat, B. Hickey, and H. Schulz (2012), Strength and geometry of the Atlantic meridional overturning circulation, *Nat. Geosci.*, *5*, 813–816.

Lynch-Stieglitz, J., et al. (2007), Atlantic meridional overturning circulation during the Last Glacial Maximum, *Science*, *316*, 66–69.

Manheim, F. T., and F. L. Sayles (1974), Composition and origin of interstitial waters of marine sediments, based on deep sea drill cores, in *The Sea*, vol. 5, edited by E. Goldberg, pp. 527–568, John Wiley, New York.

McDuff, R. E. (1984), The chemistry of interstitial waters, Deep Sea Drilling Project Leg 86, in *Initial Reports of the Deep Sea Drilling Project*, vol. 86, edited by G. R. Heath et al., pp. 675–687, U.S. Government Printing Office, Washington, D. C.

McDuff, R. E. (1985), The chemistry of interstitial waters, Deep Sea Drilling Project Leg 86, in *Initial Reports of the Deep Sea Drilling Project*, vol. 86, edited by G. R. Heath et al., pp. 675–687, U.S. Government Printing Office, Washington, D. C.

McManus, J. F., R. Francois, J.-M. Gherardi, L. D. Keigwin, and S. Brown-Leger (2004), Collapse and rapid resumption of Atlantic meridional circulation linked to deglacial climate changes, *Nature*, *428*, 834–837.

Meissner, K. J. (2007), Younger Dryas: A data to model comparison to constrain the strength of the overturning circulation, *Geophys. Res. Lett.*, *34*, L21705, doi:10.1029/2007GL031304.

Milne, G. A., and J. X. Mitrovica (2008), Searching for eustasy in deglacial sea-level histories, *Quat. Sci. Rev.*, *27*(25), 2292–2302.

Okazaki, Y., A. Timmermann, L. Menviel, N. Harada, A. Abe-Ouchi, M. O. Chikamoto, A. Mouchet, and H. Asahi (2010), Deepwater formation in the North Pacific during the Last Glacial Termination, *Science*, *329*, 200–204.

Peltier, W. R., and R. G. Fairbanks (2006), Global glacial ice volume and Last Glacial Maximum duration from an extended Barbados sea level record, *Quat. Sci. Rev.*, *25*(23), 3322–3337.

Ritz, S. P., T. F. Stocker, J. O. Grimalt, L. Menviel, and A. Timmermann (2013), Estimated strength of the Atlantic overturning circulation during the last deglaciation, *Nat. Geosci.*, *6*, 208–212.

Schmitz, W. J. (1996), On the world ocean circulation: Volume II, *Tech. Rep. 96-08*, Woods Hole Oceanographic Institution, Woods Hole, Mass.

Schrag, D. P., and D. J. DePaolo (1993), Determination of δ^{18}O of seawater in the deep ocean during the Last Glacial Maximum, *Paleoceanography*, *8*, 1–6.

Schrag, D. P., G. Hampt, and D. W. Murray (1996), Pore fluid constraints on the temperature and oxygen isotopic composition of the glacial ocean, *Science*, *272*, 1930–1932.

Schrag, D. P., J. F. Adkins, K. McIntyre, J. L. Alexander, D. A. Hodell, C. D. Charles, and J. F. McManus (2002), The oxygen isotopic composition of seawater during the Last Glacial Maximum, *Quat. Sci. Rev.*, *21*, 331–342.

Shipboard Scientific Party (1999), Site 1123: North Chatham Drift—A 20-Ma record of the Pacific Deep Western Boundary Current, in *Proc. ODP, Init. Repts*., vol. 181, edited by R. M. Carter et al., pp. 1–184, Ocean Drilling Program, College Station, Tex., doi:10.2973/odp.proc.ir.181.107.2000.

Shipboard Scientific Party (2003), Site 1239, in *Proc. ODP, Init. Repts*., vol. 202, edited by A. C. Mix et al., pp. 1–93, Ocean Drilling Program, College Station, Tex., doi:10.2973/odp.proc.ir.202.110.2003.

Skinner, L. C., S. Fallon, C. Waelbroeck, E. Michel, and S. Barker (2010), Ventilation of the deep Southern Ocean and deglacial CO_2 rise, *Science*, *328*, 1147–1151.

Srokosz, M., M. Baringer, H. Bryden, S. Cunningham, T. Delworth, S. Lozier, J. Marotzke, and R. Sutton (2012), Past, present, and future changes in the Atlantic Meridional Overturning circulation, *Bull. Am. Meteorol. Soc.*, *93*(11), 1663–1676.

Stommel, H. (1961), Thermohaline convection with two stable regimes of flow, *Tellus*, *13*(2), 224–230.

Sverdrup, H. U., M. W. Johnson, and R. H. Fleming (1942), *The Oceans: Their Physics, Chemistry, and General Biology*, vol. 7, Prentice-Hall, New York.

Talley, L. D., G. L. Pickard, W. J. Emery, and J. H. Swift (2011), *Descriptive Physical Oceanography: An Introduction*, 6th ed., 560 pp., Academic Press, Elsevier, Boston, Mass.

Toggweiler, J. R., and J. Russell (2008), Ocean circulation in a warming climate, *Nature*, *451*(17), 286–288.

WOCE Database (2013). [Available at http://woce.nodc.noaa.gov/wdiu/utils/search_tool/index.htm, Accessed January 2013.]

Wüst, G. (1935), Schichtung und Zirkulation des Atlantischen Ozeans. Die Stratophare, in *Wissenschaftliche Ergebnisse der Deutschen Atlantischen Expedition auf dem Forschungs—und Vermessungsschiff "Meteor" 1925–1927*, vol. 6, first part, 2, Walter de Gruyter & Company, Berlin.

Yokoyama, Y., K. Lambeck, P. D. Deckker, P. Johnston, and L. K. Fifield (2000), Timing of the Last Glacial Maximum from observed sea-level minima, *Nature*, *406*(6797), 713–716.

Zickfeld, K., V. K. Arora, and N. P. Gillett (2012), Is the climate response to CO_2 emissions path dependent?, *Geophys. Res. Lett.*, *39*, L05703, doi:10.1029/2011GL050205.